Computational Re-Entry Vulnerability Index Mapping to Guide Ablation in Patients With Postmyocardial Infarction Ventricular Tachycardia

Jelvehgaran, Pouya; O'Hara, Ryan; Prakosa, Adityo; Chrispin, Jonathan; Boink, Gerard J.J.; Trayanova, Natalia; Coronel, Ruben; Oostendorp, Thom

Important note
To cite this publication, please use the final published version (if applicable).
Please check the document version above.

ORIGINAL RESEARCH

VENTRICULAR TACHYCARDIA - MATHEMATICAL MODELING

Computational Re-Entry Vulnerability Index Mapping to Guide Ablation in Patients With Postmyocardial Infarction Ventricular Tachycardia

Pouya Jelvehgaran, PhD,[a,b,]* Ryan O'Hara, BSc,[c,]* Adityo Prakosa, PhD,[c] Jonathan Chrispin, MD,[d]
Gerard J.J. Boink, MD, PhD,[a,e] Natalia Trayanova, PhD,[c,]† Ruben Coronel, MD, PhD,[a,f,]† Thom Oostendorp, PhD[g,]†

ABSTRACT

BACKGROUND Ventricular tachycardias (VTs) in patients with myocardial infarction (MI) are often treated with catheter ablation. However, the VT induction during this procedure does not always identify all of the relevant activation pathways or may not be possible or tolerated. The re-entry vulnerability index (RVI) quantifies regional activation-repolarization differences and can detect multiple regions susceptible to re-entry without the need to induce the arrhythmia.

OBJECTIVES This study aimed to further develop and validate the RVI mapping in patient-specific computational models of post-MI VTs.

METHODS Cardiac magnetic resonance imaging data from 4 patients with post-MI VTs were used to induce VTs in a computational electrophysiological model by pacing. The RVI map of a premature beat in each patient model was used to guide virtual ablations. We compared our results with those of clinical ablation in the same patients.

RESULTS Single-site virtual RVI-guided ablation prevented VT induction in 3 of 9 cases. Multisite virtual ablations guided by RVI mapping successfully prevented re-entry in all cases (9 of 9). Overall, virtual ablation required 15-fold fewer ablation sites (235.5 ± 97.4 vs 17.0 ± 6.8) and 2-fold less ablation volume (5.34 ± 1.79 mL vs 2.11 ± 0.65 mL) than the clinical ablation.

CONCLUSIONS RVI mapping allows localization of multiple regions susceptible to re-entry and may help guide VT ablation. RVI mapping does not require the induction of arrhythmia and may result in less ablated myocardial volumes with fewer ablation sites. (J Am Coll Cardiol EP 2023;9:301–310) © 2023 The Authors. Published by Elsevier on behalf of the American College of Cardiology Foundation. This is an open access article under the CC BY-NC-ND license (http://creativecommons.org/licenses/by-nc-nd/4.0/).

From the ^aHeart Center, Department of Clinical and Experimental Cardiology, Amsterdam UMC, Location AMC, University of Amsterdam, Amsterdam, the Netherlands; ^bDepartment of Biomechanical Engineering, Delft University of Technology, Delft, the Netherlands; ^cAlliance for Cardiovascular Diagnostic and Treatment Innovation and Department of Biomedical Engineering, Johns Hopkins University, Baltimore, Maryland, USA; ^dDivision of Cardiology, Johns Hopkins Medical Institutions, Baltimore, Maryland, USA; ^eDepartment of Medical Biology, Amsterdam UMC, Location AMC, University of Amsterdam, Amsterdam, the Netherlands; ^fFondation Bordeaux Université, Inserm, U1045 and Université de Bordeaux, Bordeaux, France; and the ^gRadboud University Nijmegen Medical Centre, Donders Institute for Brain, Cognition and Behaviour, Nijmegen, the Netherlands. *Drs Jelvehgaran and O'Hara contributed equally to this work. †Drs Trayanova, Coronel, and Oostendorp contributed equally to this work.

The authors attest they are in compliance with human studies committees and animal welfare regulations of the authors' institutions and Food and Drug Administration guidelines, including patient consent where appropriate. For more information, visit the Author Center.

**ABBREVIATIONS
AND ACRONYMS**

CMR = cardiac magnetic
resonance imaging

MI = myocardial Infarction

RFA = radiofrequency ablation

RVI = re-entry vulnerability
index

VT = ventricular tachycardia

Patients with myocardial infarction (MI) may develop lethal re-entrant ventricular tachycardia (VT).[1] In some patients, antiarrhythmic drugs are not effective in suppressing these VTs. Radiofrequency ablation (RFA) is an effective treatment to modulate the arrhythmic substrate and prevent recurrent VT.[2,3] Precise localization of the tissue that sustains the arrhythmia is paramount to the effectiveness of RFA treatment. Mapping the VT activation pathway is used clinically to pinpoint one of multiple potential ablation targets. However, VT activation mapping requires induction of the arrhythmia that may be polymorphic, short-lasting, or hemodynamically ill tolerated. This makes sequential activation mapping not feasible. Moreover, the clinically relevant VT may not be induced during the procedure. To circumvent these drawbacks, electroanatomic mapping is performed during a paced rhythm or sinus rhythm to identify the infarct "border zone" by local low-amplitude bipolar electrograms.[4]

We previously introduced personalized 3-dimensional (3D) computational models based on the cardiac magnetic resonance imaging (CMR) of the ventricles of patients with post-MI VTs for the in silico prediction of VT ablation targets.[5,6] Although this method predicts the locations of the ablation targets that could terminate VT, it does not provide information about the multiple other VT exit sites. The RVI is a metric that can be used to detect multiple potential entry and exit sites of a re-entrant arrhythmia and, consequently, can be used to guide RFA.[7,8] The RVI metric is determined on the basis of the spatiotemporal relation between activation and repolarization times of a premature beat, and can be applied without the necessity to induce the arrhythmia.[7] Thus, generation of an RVI map has the potential to facilitate localization of myocardial tissue susceptible to RFA. Solely targeting the topmost vulnerable sites may reduce the number and extent of ablations and shorten the procedure time.

We aimed to assess whether RVI mapping based on a single premature beat can detect multiple vulnerable regions using personalized 3D left ventricular image-based models of patients with post-MI VTs.[5,6] We expected that a single simulated ablation of the topmost vulnerable region would only be partially effective in preventing VT, because of the presence of multiple exit sites of the VT circuit, and that ablations of the combined topmost vulnerable regions would be more effective. We demonstrated the feasibility of a novel, noninvasive approach based on the RVI metric

using patient-specific computational models to enhance the guidance of clinical RFA.

METHODS

PERSONALIZED COMPUTATIONAL HEART MODELING.
We studied 4 patients with post-MI monomorphic VTs (mean age 67.2 ± 11.7 years; 1 woman) from recent studies on ablation of infarct-related VT.[5,9] Patients underwent preablation cardiac late gadolinium enhancement CMR and subsequent clinical RFA.[5] The Johns Hopkins Institutional Review Board approved sharing of deidentified patient data with the modeling team for the retrospective study. Given the retrospective nature of the study, the Institutional Review Board did not require patient informed consent.

PACING AND VT INDUCTION. For each of the 4 patients, a virtual heart model was created based on the CMR images (Supplemental Figure 1). Electrophysiological characteristics were attributed to normal tissue, scar tissue, and gray-zone tissue.[5] A validated pacing protocol was used to generate VT.[5] Seven pacing locations were evenly distributed in each model (3 basal, 3 midmyocardial, and 1 apical) and in proximity of gray zone. At each site, pacing (6× S1, cycle length 600 milliseconds) followed by a premature stimulus (S2, coupling interval of 300 milliseconds). The S1-S2 coupling interval was decreased in steps of 10 milliseconds until failure to capture. Additional successive premature stimuli (S3/S4/S5) were delivered at a coupling interval of 250 milliseconds. Sustained re-entry was simulated for 5 seconds. For each VT, we identified the re-entrant circuit through visual analysis. If re-entry did not occur following S5 pacing, we considered the model noninducible from that specific pacing site.

VIRTUAL ABLATION GUIDED BY THE RVI MAPS. The RVI is a quantitative spatial[7,10] that predicts whether a premature activation wave front is capable of inducing re-entry based on a S1-S2 pacing at a particular location (see schematic in Supplemental Figure 2). The novelty of the RVI metric is that it allows detection of multiple arrhythmogenic locations (RFA ablation targets) without the need to induce arrhythmias. The RVI was calculated for the activation/repolarization patterns of each pacing site of the 4 patient models with induced re-entry. For the calculation of the RVI map, only the S2 beat was used. The S2 stimulus alone did not lead to re-entry in any of the cases. A low RVI value indicates high vulnerability to re-entry (Supplemental Appendix).

Based on the RVI map virtual ablations were implemented in the model as nonconducting hemispheres intersecting with the elements of the 3D ventricular heart model centered on the identified node.[5] To evaluate the RVI method, we used 2 virtual ablations approaches in the ventricular heart models based on the RVI map(s) generated for each patient per pacing site: 1) single-site ablation—with a hemisphere of 10 mm in diameter—was applied to the node with the lowest RVI; and 2) because the RVI method ranks the susceptibility of each node to re-entry, we virtually ablated up to 15 nodes with the lowest RVI values in 1 session, replicating clinical RFA methods (multisite ablation).[6] We excluded virtual ablations that would render the pacing site inexcitable.

Virtual ablations were performed starting with hemispheres of up to 4 mm in diameter at the RVI nodes with the lowest RVI and—if the virtual ablation could not terminate the re-entry—subsequently 10, and 15 RVI nodes with the lowest RVI value, for each pacing site. In some cases, other targeted nodes were within the diameter of the virtual ablation, which resulted in less ablated myocardium than when the RVI nodes were further apart.

The virtually ablated ventricular heart models (Supplemental Figure 3) were subjected to the rapid pacing protocol to test whether the virtual ablations prevented VT induction. Ablation success was defined by absence of an arrhythmia following 4 premature beats.

Virtual ablations analysis. We compared our virtual ablation results guided by the RVI (based on the second approach) to the clinical ablation procedure of the same patient. For each virtual ablation, the number of ablations and the fraction of the left ventricular mass was calculated (based on the catheter positions and the CMR-based ventricular model) and compared with the fraction that was ablated in the actual ablation procedure in these patients. The geodesic distance was calculated between the VT isthmus and the first and second lowest RVI nodes as well as between the pacing location and the VT isthmus using the surface mesh from each pacing site. The fast-marching algorithm was used to find the shortest path along the nodes of each mesh using a set of starting points.[11] Data are presented as mean ± SD (range).

RESULTS

In 4 patient models, 9 different sustained VTs were induced from 9 pacing sites (Video 5). RVI maps were calculated for the S2 beats of the corresponding in-

duction protocols (none of the S2-activation induced VT). The RVI maps calculated for the 4 patient-specific models contained an average of 481,186 ± 120,284 nodes (range 316,122-588,120 nodes).

Figure 1A shows activation maps after the left ventricular myocardium stimulation in a post-MI VT of patient 2. Movies of the initiation of the VT are available in the supplementary materials (Videos 1-4). The still of the Video shows late activation (red) in the isthmus of the VT and the re-entrant pattern leading into the next activation map. The **arrow** pointing to the VT isthmus indicates the vulnerable region. **Figure 1B** shows the RVI map, derived from the ATs and RTs pertaining to stimulation (S2) delivered at the site indicated by the star. The 2 blue hemispheres indicate the 2 locations where the RVI has a local minimum. Note that one is exactly located at the VT isthmus, and the other is located in the re-entrant pathway. We next measured the distance between the VT isthmus and the corresponding RVI minimum in all cases of VT induction. The average distance between the RVI minimum and the VT isthmus was 13.26 ± 9.97 mm (n = 9).

RVI-GUIDED ABLATION. Single virtual ablation. **Figures 2A to 2C** show images of the RVI map, in which the lowest RVI is highlighted at the basal inferior wall (patient 1). A single simulated ablation with a hemispheroid area (of 10 mm in diameter) at that site resulted in failure to induce the VT.

Table 1 presents the virtual ablation results of the lowest RVI at 10 mm for all patients and pacing locations. A single virtual ablation of 10 mm in diameter was successful in 3 of 9 cases. In 1 unsuccessful case (patient 1, paced from the basal inferoseptal wall) the lowest RVI was very close (1.17 mm) to the VT isthmus, but the virtual single ablation was unable to prevent the re-entry.

The overall virtual ablation fraction and the fraction of conducting tissue ablated on average were 1.46% ± 0.42% and 0.98% ± 0.37%, respectively.

Multiple virtual ablations. **Figures 2D to 2F** present an example of RVI-guided virtual ablation in patient 4 after S2 pacing from the mid anteroseptal wall. Ablations were executed node with the lowest RVI as well as the 15 subsequent RVI nodes. The second-lowest RVI value in the RVI surface map identified the susceptible region of the re-entrant pathway induced by pacing from this location. Virtual ablation at 4 mm of the lowest 15 RVI nodes successfully prevented VT induction following rapid pacing. The VT exit site in this patient occurs in the basal region (arrow in **Figure 2E**) and virtual ablation of the 9 lowest RVI nodes—excluding of 1 at the pacing site—is shown in

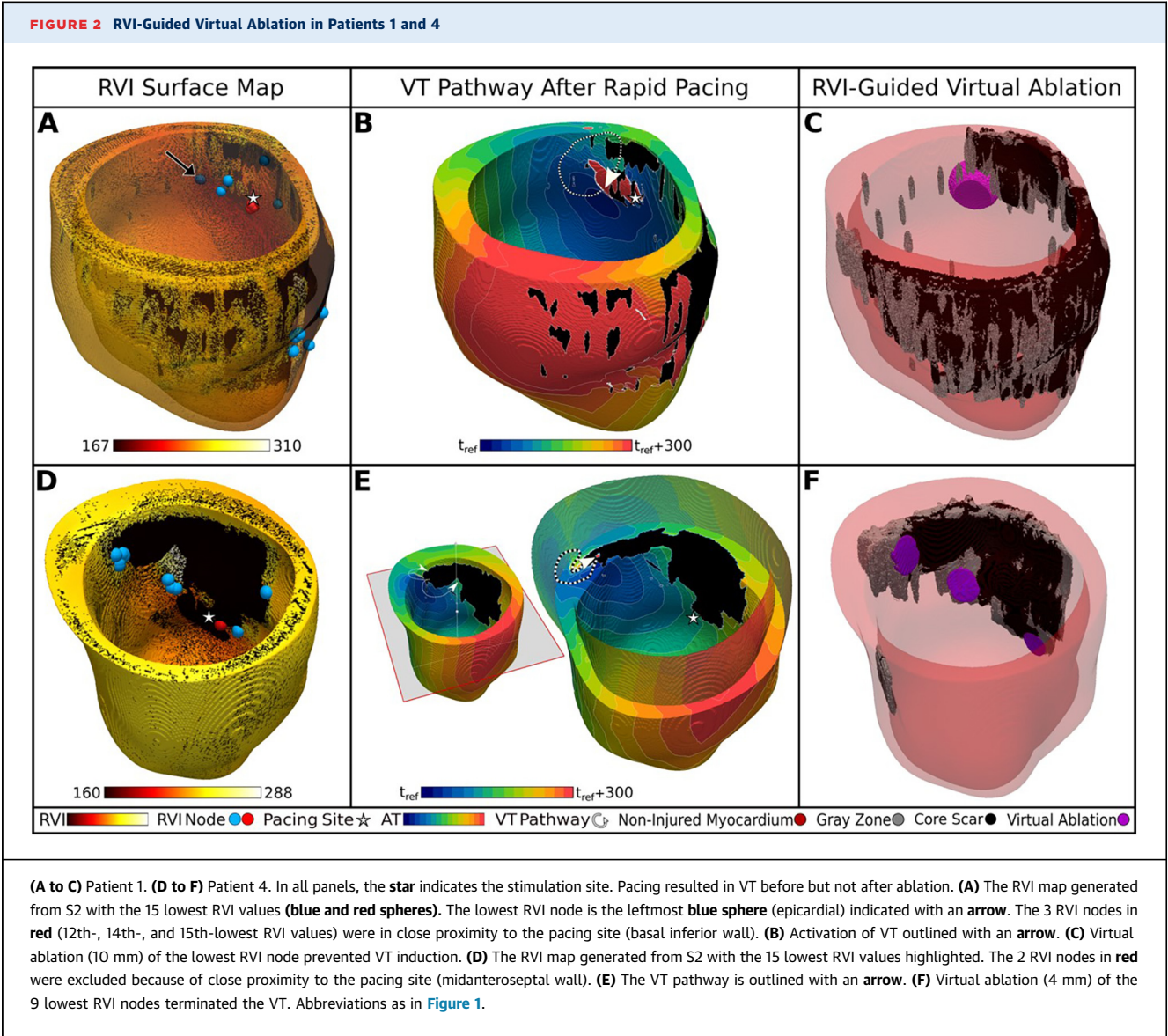**FIGURE 1 Activation Maps and RVI Map of VT Exit Sites**
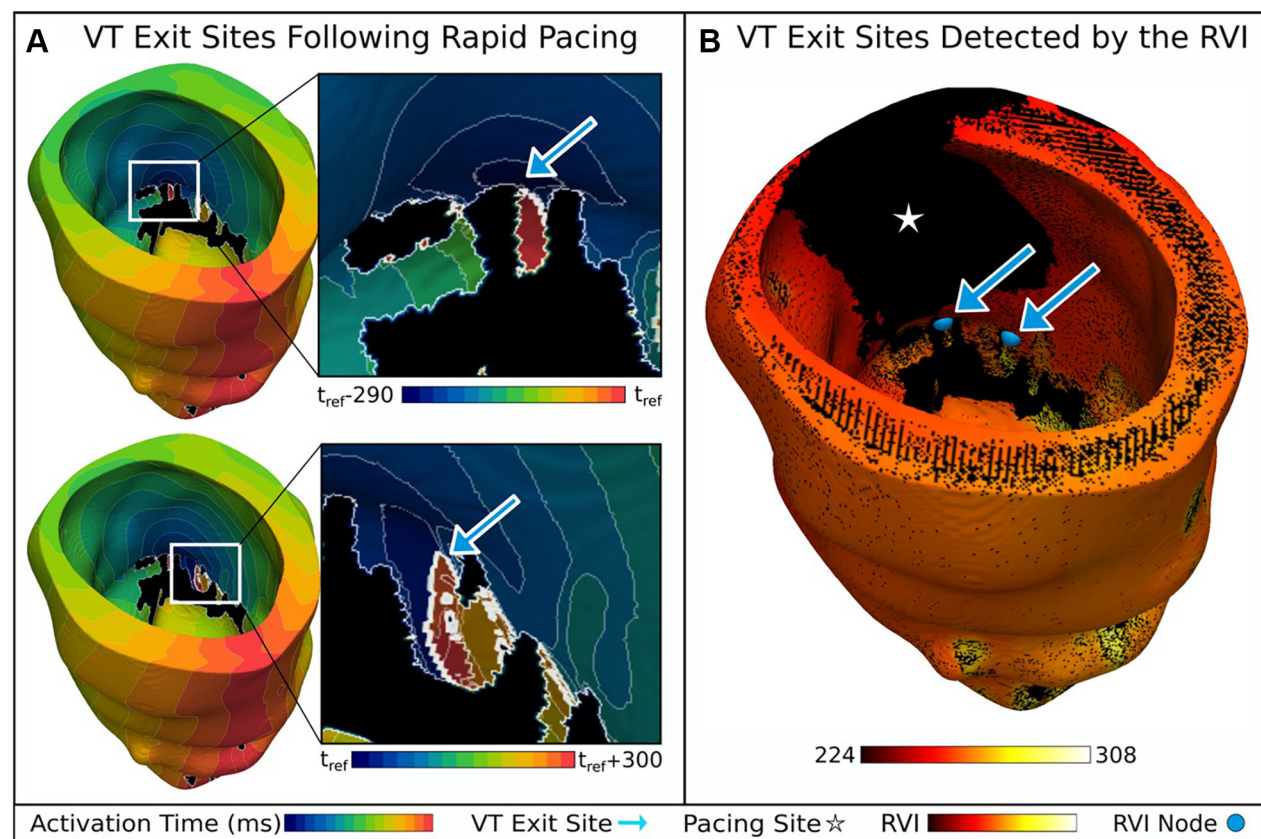
(A) Simulated 3-dimensional activation maps in a patient-specific model of left ventricular wall during 2 ventricular tachycardia (VT) activations **(boxes: zoomed-in areas)**. **Black** indicates scar. Two exit sites are indicated by **arrows** (Video 3). **(B)** The re-entry vulnerability index (RVI) map of the same heart as in **A** calculated following S2. Tissue surrounding the pacing site **(star)** has been excluded (see Methods section). Scar tissue is apical (compare with **A**). The first **(left)** and fourth ranked **(right)** nodes of the lowest RVI values are indicated with **blue spheres**. The second- and third-lowest RVI nodes (not visible in the figure) are located on the midinferior wall. **Arrows** point to the corresponding sites in **A**.

Figure 2F. In this example, virtual ablation resulted in VT prevention and in removal of 1.03% of conducting tissue.

Overall, we performed an average of 10.9 ± 2.9 virtual ablations per pacing condition (10.46 ± 1.47 per patient) and ablated 1.17% ± 0.27% of conducting tissue per pacing condition (1.36% ± 0.41% per patient) to prevent induction of all of the VTs (**Table 2**). Thus, the multiple virtual ablations guided by the RVI were able to terminate the re-entry in 9 of 9 cases. Videos from before and after virtual ablation are provided in the Supplemental Figure 3.

We next analyzed the location of the 15 nodes with the lowest RVI values for each RVI map. In all 9 RVI maps, the 15 nodes with the lowest RVI values were located in regions of gray zone. **Figure 3A** shows the RVI map for patient 1 containing the 15 epicardial and endocardial nodes with the lowest RVI values that were subsequently mapped onto the fibrotic remodeled tissue (**Figure 3B**). **Table 3** shows a summary of the lowest RVI nodes in each RVI map and how they appeared as clusters. The VT exit sites were correctly identified among the top 15 ranking nodes (mean 5.1 ± 4.6 nodes, range 1-15 nodes) with the lowest RVI values for each inducible pacing site of the 4 ventricular heart models. Additionally, when considering clusters of the lowest 15 RVI nodes (<1 mm apart) in each RVI map, the VT exit sites were correctly identified among the average 3.8 ± 2.7 clusters (range 1-8 clusters) with the lowest RVI values. The RVI detected multiple regions of arrhythmia susceptibility within the same patient across multiple locations without the need for repeated VT induction. Of the 15 nodes with the lowest RVI values considered for each

FIGURE 2 RVI-Guided Virtual Ablation in Patients 1 and 4

(A to C) Patient 1. **(D to F)** Patient 4. In all panels, the **star** indicates the stimulation site. Pacing resulted in VT before but not after ablation. **(A)** The RVI map generated from S2 with the 15 lowest RVI values **(blue and red spheres)**. The lowest RVI node is the leftmost **blue sphere** (epicardial) indicated with an **arrow**. The 3 RVI nodes in **red** (12th-, 14th-, and 15th-lowest RVI values) were in close proximity to the pacing site (basal inferior wall). **(B)** Activation of VT outlined with an **arrow**. **(C)** Virtual ablation (10 mm) of the lowest RVI node prevented VT induction. **(D)** The RVI map generated from S2 with the 15 lowest RVI values highlighted. The 2 RVI nodes in **red** were excluded because of close proximity to the pacing site (midanteroseptal wall). **(E)** The VT pathway is outlined with an **arrow**. **(F)** Virtual ablation (4 mm) of the 9 lowest RVI nodes terminated the VT. Abbreviations as in **Figure 1**.

pacing site, the cumulative number of unique clusters per patient was 7.2 ± 1.0 despite the individual average of each RVI map containing 9.6 ± 2.7 unique clusters ($P < 0.05$), indicating that multiple susceptible regions can be identified using the RVI method from different pacing locations.

The RVI minimum cluster was unique for all cases, except in patient 1, where the RVI map calculated following pacing from the midlateral wall identified the same RVI minimum following pacing at the basal inferior wall. This RVI minimum identified the primary exit site of one VT morphology, but not the other. However, both exit sites were identified by each RVI map when considering up to the 15 nodes

with the lowest RVI values. The application of multiple stimulation sites allowed identification of more exit sites than pacing from a single stimulation site. Pacing from various sites also identified the same RVI-minima.

NUMBER AND TOTAL VOLUME OF ABLATION SITES. Table 4 shows both the virtual ablation results guided by the RVI (multiple ablation approach), as well as the clinical ablation results for each patient. The overall virtual ablation fraction was 2-fold lower than the clinical ablation fraction. On average, the overall number of virtual ablations was 17 ± 6.8 (range 9-24) compared with 253.5 ± 97.4 clinical

TABLE 1   Ablation of Lowest RVI Node at 10 mm

ID	LV Pacing Location	Re-Entry-Inducing Premature Stimuli	10 mm Ablation of Lowest RVI Node Prevented Re-Entry?	Virtual Ablation Fraction (%)	Fraction of Conducting Tissue Ablated (%)
1	Mid lateral	S5	No	1.62	0.94
	Basal inferoseptal	S4	No	1.21	0.32
	Basal inferior	S5	Yes	1.09	0.92
2	Basal anteroseptal	S3	No	1.71	1.34
	Mid anteroseptal	S3	Yes	1.29	0.61
3	Mid lateral	S3	No	1.41	1.29
	Mid inferior	S3	Yes	1.29	0.98
	Apex	S3	No	1.09	0.92
4	Mid anteroseptal	S3	No	2.42	1.51

LV = left ventricular; RVI = re-entry vulnerability index.

ablations (range 128-356 clinical ablations). Hence, the virtual ablation guided by the RVI required nearly 15-fold fewer ablations than what was applied clinically.

DISCUSSION

In this simulation study based on patient-specific modeling of the left ventricular walls of patients with postinfarction VTs, we demonstrate the ability of the RVI to localize multiple regions susceptible to re-entry and to guide ablation of these regions to prevent re-entrant VT (**Central Illustration**). We show that the sites with the 15 lowest RVIs colocalize with the susceptible part of a VT circuit. Virtual ablation of these sites led to noninducibility of the VT. Our method to localize ablation targets is based on CMR and is therefore noninvasive. The calculated ablation volume is smaller than clinically achieved, and would be clinically faster to perform caused by fewer ablations. Moreover, because RVI mapping localizes multiple vulnerable sites at the time, repeated

inductions and activation mapping of a VT is not necessary. Thus, the RVI mapping may help guide ablation therapy to prevent VT. Our method adds mechanistic information to repolarization mapping of infarcted myocardium.[12]

We earlier introduced the RVI concept as a quantitative measure interval that predicts whether a premature activation wave front is capable of inducing re-entry.[7,10] The novelty of the RVI method is that it allows detection of multiple arrhythmogenic locations (RFA targets), without the need to induce arrhythmias.[7,10] Existing mapping techniques require induction of the clinically relevant VT in the sedated patient. Furthermore, sequential mapping demands the presence of a sustained, monomorphic VT. This is not always possible, is not always tolerated, or is very time-consuming. RVI mapping, whether intraprocedural or preprocedural, in combination or not with modelling (as in the present work) avoids these drawbacks, because VT induction is not necessary (a single, not critically coupled premature beat suffices) and identifies multiple susceptible sites of the re-entrant circuit(s).

Only the first premature activation was used to calculate RVI, and no arrhythmia was induced. Our results indicate that single ablation of the site with the minimum RVI is successful in preventing VT in about 33% of cases. This is consistent with the pathophysiology of post-MI VTs, where multiple susceptible regions and VT circuits may exist in 1 heart, and multiple VT morphologies can exist in 1 patient. Ablation of a single site, therefore, may unmask a secondary VT pathway. Thus, multiple ablation lesions are required to prevent VT induction. We show that the top 15 ranked RVI sites were able to prevent all VTs in all patients. In addition, the overlap of the identified RVI clusters confirms that the same susceptible regions can be identified by the metric

TABLE 2   Ablation of 5, 10, or 15 Lowest RVI Nodes at 4 mm

ID	Pacing Location	Re-Entry-Inducing Premature Stimuli	RVI Nodes Considered for Virtual Ablation	Re-Entry Prevented	No. of Virtual Ablations	Virtual Ablation Fraction (%)	Fraction of Conducting Tissue Ablated (%)
1	Mid lateral	S5	15 lowest at 4 mm	Yes	15	1.36	0.59
	Basal inferoseptal	S4	15 lowest at 4 mm	Yes	15	1.24	0.56
	Basal inferior	S5	10 lowest at 4 mm	Yes	10	0.87	0.38
2	Basal anteroseptal	S3	10 lowest at 4 mm	Yes	6	0.57	0.35
	Mid anteroseptal	S3	15 lowest at 4 mm	Yes	13	1.18	0.82
3	Mid lateral	S3	10 lowest at 4 mm	Yes	10	0.92	0.7
	Mid inferior	S3	10 Lowest at 4 mm	Yes	10	0.82	0.49
	Apex	S3	10 lowest at 4 mm	Yes	10	1.37	1.08
4	Mid anteroseptal	S3	10 lowest at 4 mm	Yes	9	1.41	1.03

RVI = re-entry vulnerability index.

FIGURE 3 Example of RVI Calculation Following S2 at the Midlateral Wall

(A) Generated re-entry vulnerability index (RVI) map. **Black** regions represent scar or no data. (B) The 15 nodes with the lowest RVI values mapped onto the fibrotic tissue.

calculated based on different pacing sites. Our results showed that the RVI metric could find multiple clusters of the lowest RVI values from a single pacing location. This is expected as single RVI calculation should yield multiple if not all VT susceptible regions. It is consistent with the concept that post-MI VTs can arise from multiple pathways that use shared myocardial strands.[13,14] Adding more pacing locations may identify additional susceptible sites (but with duplicates). In a minority of cases, a single ablation alone could prevent re-entry. The secondary conduction pathways may be used for re-entrant activation after each ablation. We demonstrate that up to 10 clusters can be identified by a single RVI calculation and that the top 15 ranked (lowest RVI values) were able to prevent VTs in all patients.

Our findings support the preprocedural use of RVI mapping to guide ablation procedures in clinical practice of post-MI VT and in other cases of re-entry-based arrhythmias. Peroperative RVI mapping

TABLE 3 RVI Detection of VT Exit Sites

ID	No. of Nodes in the RVI Map	Pacing Location	Unique RVI Clusters (Nodes <1 mm Apart—Lowest 15 Nodes)	Lowest RVI Node that Identified the Primary Exit Site	Lowest RVI Cluster that Identified the Primary Exit Site	Cumulative Unique Clusters
1	588120	Mid lateral	13	9	8	22
		Basal inferoseptal	12	1	1	
		Basal inferior	11	4	3	
2	471302	Basal anteroseptal	7	1	1	12
		Mid anteroseptal	6	15	6	
3	549200	Mid lateral	9	7	7	25
		Mid inferior	10	1	1	
		Apex	12	5	4	
4	316122	Mid anteroseptal	6	3	3	6

RVI = re-entry vulnerability index.

TABLE 4 Comparison

ID	Gender	Age, y	No. of Clinical Ablation Sites	LV Volume (mL)	Clinical Ablation Volume (mL)	Clinical Ablation Fraction (%)	No. of Virtual Ablations	Virtual Heart Volume (mL)	Virtual Ablation Volume (mL)	Virtual Ablation Fraction (%)
1	Male	67	356	147.02	5.68	3.87	24	146.37	3.81	2.60
2	Male	85	296	135.74	5.97	4.4	14	135.61	2.31	1.70
3	Male	69	128	144.38	6.93	4.8	21	144.14	3.91	2.71
4	Female	62	234	63.72	2.77	4.35	9	63.63	0.90	1.41

Abbreviations as in **Table 1**.

may confirm or replace the preprocedural noninvasive approach. The modelling part of the method may be replaced by noninvasive electrocardiographic imaging to generate patient-specific RVI maps. A previous clinical study has described the accuracy of sequential RVI catheter mapping to localizing VT exit sites. Our study adds the effectiveness of virtual ablation, the existence of overlapping clusters of minimum RVI, and the effect of multiple pacing locations.[15]

In silico modelling of patient specific heart models of the left ventricle has been used before to identify ablation targets.[5,6,16] However, it necessitates multiple, sequential, time-consuming inductions of the VT followed by addition of ablation lesions to identify subsequent ablation targets. Incorporation of RVI mapping (where only 1 cycle needs to be analyzed) may reduce calculation time, and thus, accelerate the process. Real-time RVI mapping during clinical electrophysiological VT mapping requires the incorporation of RVI mapping into mapping algorithms and is feasible.

In this study, each pacing location leads to a unique VT morphology and a corresponding set of

CENTRAL ILLUSTRATION Procedure and Result of Computational Re-Entry Vulnerability Mapping
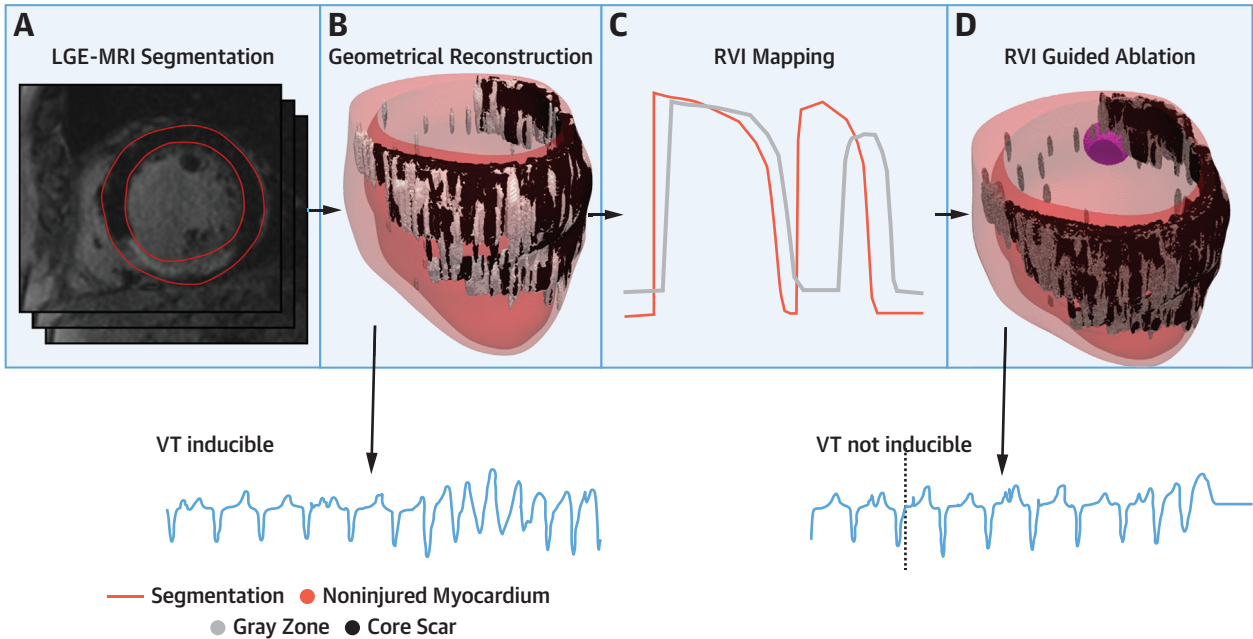
Jelvehgaran P, et al. J Am Coll Cardiol EP. 2023;9(3):301–310.

Based on LGE-MRI **(A)** a segmentation of the left ventricle is made, including core scar and 'gray zone' **(B)**. Electrophysiological characteristics are assigned to the three regions (core scar, gray zone and normal myocardium) and the heart is paced in silico **(C**, schematic action potentials shown). Based on a single paced premature activation **(C)**, the Re-entry vulnerability index (RVI) was calculated at each node and mapped on the heart model. A myocardial location sensitive to ablation was identified **(D, purple sphere)**. After virtual ablation at that site, VT was no longer inducible (schematic unipolar electrograms shown).

RVI clusters (Table 3). Pacing from one location vs another leads to considerable cluster overlap in patient 1 (36 clusters from 3 pacing sites, with 22 unique clusters total), although this could differ between patients (less overlap in patient 2). The overlap of clusters is likely dictated by the wave front direction and geometry of the remodeled myocardium. Here, we calculated the RVI derived from the same pacing location that resulted in VT. When the VT circuits are unknown, more pacing sites (7 have been used most recently) may be required.

The number of pacing locations required to identify the necessary clusters would depend on the amount and distribution of the remodeled myocardium. We can pace from as many locations as there are nodes in the models, but the computational cost and time would outweigh the benefit.

The spatial resolution of our ventricular models was much higher than can be achieved with clinical mapping. RVI mapping has, however, been applied using a lower spatial resolution.[8] Hence, even with a lower spatial resolution, RVI mapping can identify the isthmus of a re-entrant VT.

STUDY LIMITATIONS. In post-MI VTs, the substrate for re-entry is formed by the structural changes of the infarcted tissue. Although our model was restricted to the left ventricular myocardium and other structures may be important for arrhythmogenesis, it reliably represents the VT substrate, and ablation based on tissue-specific arrhythmia simulation is clinically effective as well.[5,6]

We assumed that a border zone exists around the infarcted tissue and that conduction slowing can be attributed to this zone. However, this is not necessarily the case, because the conduction delay in post-MI tissue is caused by tortuosity of the activation path.[14] Nevertheless, using this simplification, we simulated VTs that resembled the clinical cases.

We used 10 mm for the ablation lesion diameter in the first approach. Even with this relatively large size, we documented that RVI-guided ablation resulted in smaller lesion volume for the successful cases than what was clinically observed. The average lesion size in clinical studies was 1.4 ± 1.4 mL, with a mean endocardial region of 3.5 ± 3.0 cm^2.[17]

CONCLUSIONS

We demonstrated the feasibility of in silico RVI mapping to detect multiple regions susceptible to re-entry without VT induction using patient-specific

image-based models of the left ventricle from patients with MI and monomorphic VT. RVI mapping successfully allowed guidance of simulated ablation. The success rate of virtual RVI-guided multisite ablation was 100%. Comparison with retrospective clinical ablation data showed that RVI-guided ablation can lead to a reduction of the volume of the ablated tissue and of the number of ablation sites. We surmise that our approach can be translated to the clinical practice to guide ablation in patients with post-MI VTs.

ADDRESS FOR CORRESPONDENCE: Dr Pouya Jelvehgaran OR Dr Ruben Coronel, Heart Center, Department of Clinical and Experimental Cardiology, Amsterdam UMC, Location AMC, University of Amsterdam, Meibergdreef 9, 1105 AZ Amsterdam, the Netherlands. E-mail: p.jelvehgaran@amsterdamumc.nl OR rubencoronel@gmail.com.

PERSPECTIVES

COMPETENCY IN MEDICAL KNOWLEDGE: Combined activation-repolarization RVI mapping in patient-specific in silico models identifies re-entry–sensitive tissue (isthmus, exit sites) and allows for guiding low-volume tissue ablation in patients with post-MI VTs, without the need to induce re-entrant arrhythmia during the ablation procedure. This work also suggests that peroperative in-patient RVI mapping is feasible and may shorten and promote selective ablation approaches.

TRANSLATIONAL OUTLOOK: Combined activation and repolarization mapping, requiring analysis of unipolar electrograms, makes it possible to identify exit sites of a VT in post-MI patients without the need to induce the re-entrant arrhythmia. The RVI algorithm can be incorporated into existing mapping systems.

REFERENCES

1. Koplan BA, Stevenson WG. Ventricular tachycardia and sudden cardiac death. *Mayo Clin Proc*. 2009;84:289–297.

2. Shivkumar K. Catheter ablation of ventricular arrhythmias. *N Engl J Med*. 2019;380:1555–1564.

3. Tung R, Vaseghi M, Frankel DS, et al. Freedom from recurrent ventricular tachycardia after catheter ablation is associated with improved survival in patients with structural heart disease: an International VT Ablation Center Collaborative Group study. *Heart Rhythm*. 2015;12:1997–2007.

4. Santangeli P, Marchlinski FE. Substrate mapping for unstable ventricular tachycardia. *Heart Rhythm*. 2016;13:569–583.

5. Prakosa A, Arevalo HJ, Deng D, et al. Personalized virtual-heart technology for guiding the ablation of infarct-related ventricular tachycardia. *Nat Biomed Eng*. 2018;2:732–740.

6. Arevalo HJ, Vadakkumpadan F, Guallar E, et al. Arrhythmia risk stratification of patients after myocardial infarction using personalized heart models. *Nat Commun*. 2016;7:11437. https://doi.org/10.1038/ncomms11437

7. Coronel R, Wilms-Schopman FJG, Opthof T, Janse MJ. Dispersion of repolarization and arrhythmogenesis. *Heart Rhythm*. 2009;6:537–543.

8. Child N, Bishop MJ, Hanson B, et al. An activation-repolarization time metric to predict localized regions of high susceptibility to reentry. *Heart Rhythm*. 2015;12:1644–1653.

9. Deng D, Prakosa A, Shade J, Nikolov P, Trayanova NA. Sensitivity of ablation targets prediction to electrophysiological parameter variability in image-based computational models of ventricular tachycardia in post-infarction patients. *Front Physiol*. 2019;10:1–12.

10. Coronel R, Wilms-Schopman FJ, Janse MJ. Anti- or profibrillatory effects of Na(+) channel blockade depend on the site of application relative to gradients in repolarization. *Front Physiol*. 2010;1:10.

11. Peyré G, Cohen L. Geodesic remeshing using front propagation. *Int J Comput Vis*. 2006;69:145–156.

12. Callans DJ, Donahue JK. Repolarization Heterogeneity in Human Post-Infarct Ventricular Tachycardia. *J Am Coll Cardiol EP*. 2022;8:713–718.

13. Stevenson WG, Khan H, Sager P, et al. Identification of reentry circuit sites during catheter mapping and radiofrequency ablation of ventricular tachycardia late after myocardial infarction. *Circulation*. 1993;88:1647–1670.

14. de Bakker JM, van Capelle FJ, Janse MJ, et al. Slow conduction in the infarcted human heart. "Zigzag" course of activation. *Circulation*. 1993;88:915–926.

15. Orini M, Graham AJ, Srinivasan NT, et al. Evaluation of the reentry vulnerability index to predict ventricular tachycardia circuits using high-density contact mapping. *Heart Rhythm*. 2020;17:576–583.

16. Deng D, Prakosa A, Shade J, Nikolov P, Trayanova NA. Sensitivity of ablation targets prediction to electrophysiological parameter variability in image-based computational models of ventricular tachycardia in post-infarction patients. *Front Physiol*. 2019;10:628. https://doi.org/10.3389/fphys.2019.00628

17. Ilg K, Baman TS, Gupta SK, et al. Assessment of radiofrequency ablation lesions by CMR imaging after ablation of idiopathic ventricular arrhythmias. *J Am Coll Cardiol Img*. 2010;3:278–285.

APPENDIX For an expanded Methods section as well as supplemental videos and figures, please see the online version of this paper.